THE EUROPEAN
PHYSICAL JOURNAL B

Regular Article

Indirect control of spin precession by electric field via spin-orbit coupling

Li-Ping Yang[1,2,a] and Chang-Pu Sun[2,3]

[1] State Key Laboratory of Theoretical Physics, Institute of Theoretical Physics and University of the Chinese Academy of Sciences, Beijing 100190, P.R. China
[2] Synergetic Innovation Center of Quantum Information and Quantum Physics, University of Science and Technology of China, Hefei, Anhui 230026, P.R. China
[3] Beijing Computational Science Research Center, Beijing 100084, P.R. China

Abstract. Spin-orbit coupling (SOC) can mediate the electric-dipole spin resonance (EDSR) within an a.c. electric field. By applying a quantum linear coordinate transformation, we find that the essence of EDSR could be understood as a spin precession under an effective a.c. magnetic field induced by the SOC in the reference frame, which is following exactly the classical trajectory of this spin. Based on this observation, we find an upper limit for the spin-flipping speed in the EDSR-based control of spin. For two-dimensional case, the azimuthal dependence of the effective magnetic field can be used to measure the ratio of the Rashba and Dresselhaus SOC strengths.

1 Introduction

It is of great importance to prepare and manipulate the pure quantum state of single particles for quantum information processing and even for the future quantum devices using the new degrees of freedom, such as the spin. Through Coulomb blockade, the single electron state in the charge degree of freedom has been realized in a quantum dot (QD) system [1–8]. In the last decade, the spintronics provides a new paradigm for quantum operations of spin in addition to the electric charge [9,10]. However, the issue of how to perfectly control the quantum state of a single spin in a QD is still challenging.

The conventional method to flip the spin is based on the electron spin resonance (ESR) [11], where resonant magnetic field pulses are applied. Different from an a.c. electric field, which could be generated by exciting a local gate electrode, a strong and high-frequency magnetic field is very difficult to apply effectively to a micro/nanostructure with a QD [12,13]. To overcome this problem, physicists try to control electron spin in another fashion with an electric field. Rashba and Efros [14,15] proposed to realize indirect control of the electron spin by electric field through spin-orbit coupling (SOC) [16,17]. With SOC, the moving electron spin seems to experience an additional effective magnetic field induced by the a.c. electric field. When the frequency of the electric field matches the Zeeman splitting of the electron spin, the coherent control of a single electron spin can be achieved with an electric

field indirectly [18–23]. This spin resonance in the effective magnetic field is called electric-dipole spin resonance (EDSR) [24].

There is a lot of literature [25–29] on the theoretical explanation of EDSR effects. An intuitive picture of EDSR is given by Golovach et al. [25]. They first eliminated the SOC terms by making the Schrieffer-Wolff transformation to the first order of perturbation theory, and then they found that the electric field would behave as an effective magnetic field. In this paper, we revisit this enlightening physical explanation by studying the spin dynamics in a reference frame which follows exactly the classical trajectory of a driven electron trapped in a harmonic potential. For a QD in a one-dimensional (1D) nanowire, the electron is constrained in a harmonic trap and driven by an a.c. electric field. When the trap is tight enough, the influence of the high-frequency free oscillation of the electron on the dynamics of the spin can be neglected, but the forced oscillation of the electron under the a.c. electric field with lower frequency provides the spin with an effective resonant magnetic field through SOC. If the a.c. electric field is along the axis of the wire, the magnetic field induced by Rashba SOC is perpendicular to the electric field, while the one induced by Dresselhaus SOC is parallel to the electric field. The induced magnetic field has the same frequency as the driving electric field, and the coherent controlling of the spin can then be realized when the electric field is resonant with the Zeeman splitting (ω_z) of the electron spin. Our investigation here shows that for a tight trap, one can enlarge the Zeeman splitting of the

[a] e-mail: `lipingyang@csrc.ac.cn`
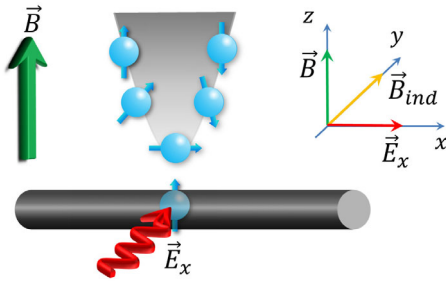
Fig. 1. The electron moving in a one-dimensional nanowire is constrained in a harmonic trap. The electron spin is initially polarized along the z-axis by an external static magnetic field $\boldsymbol{B}$. When an a.c. electric field $\boldsymbol{E}_x(t)$ is applied to drive the electron, the electron spin will experience an additional magnetic field induced by the SOC. In our case, the magnetic field induced by Rashba SOC is perpendicular to the electric field.

electron spin, in addition to increasing SOC strength or electric driving strength, to increase the spin-flip speed. But there exists an upper limit ($\sim 10^{-2}\omega_z$) of the effective Rabi frequency of the coherent control of the spin with EDSR [30].

For a two-dimensional (2D) QD system, we find that the induced a.c. magnetic field becomes azimuth dependent. If the external static magnetic field is weak and the 2D harmonic trap is isotropic, we discover that the magnetic field induced by Rashba SOC is still perpendicular to the electric field. The a.c. magnetic field induced by Dresselhaus SOC lies on the mirror-image line of the a.c. electric field with respect to the x-axis. Based on the above understanding of the EDSR, we can realize the precise control of spin precession on the Bloch sphere surface. On the other hand, we can also measure the ratio of the Rashba and Dresselhaus SOC strengths by using the azimuthal dependence of the induced magnetic field as proposed in reference [15].

In the next section, we present our model and show the origin of the effective magnetic field in EDSR. In Section 3, the effective spin precession under the electric field through SOC is presented. We investigate how to speed up the coherent spin control with EDSR in Section 4. In Section 5, we study the coherent spin control via EDSR in a 2D QD system. Finally, the summary of our main results is given in Section 6. Some detailed calculations are displayed in the Appendices.

2 The electric-dipole spin resonance

We first take the 1D nanowire QD system, where an electron is confined in an 1D harmonic trap along the x-direction with frequency ω (Fig. 1), as an illustration to explore the physical mechanism of EDSR. The model Hamiltonian reads [31,32],

$$H = \hbar\omega a^\dagger a - i\tilde{\alpha}\left(a^\dagger - a\right)\sigma_y + \frac{1}{2}\hbar\omega_z\sigma_z + \xi\left(a^\dagger + a\right)\cos\nu t,$$ (1)

where $a = \sqrt{m_e\omega/(2\hbar)}[x + ip_x/(m_e\omega)]$ is the annihilation operator of the vibration degree of the electron with coordinate (momentum) x (p_x) and the effective mass m_e, $\tilde{\alpha} = \alpha\sqrt{m_e\omega/(2\hbar)}$ with the Rashba SOC constant α, $\xi = eE_x\sqrt{\hbar/(2m_e\omega)}$ is the effective driven strength of the a.c. electric field $-E_x\cos\nu t$. An external static magnetic field with strength B is applied along the z-direction to polarize the electronic spin. $\omega_z = g\mu_B B/\hbar$ is the Zeeman splitting of the electron spin with the Bohr magneton μ_B and the effective g-factor g. Here, we just take the Rashba SOC into account, because our approach can be generalized to the Dresselhaus case straightforwardly. Hereafter, we take $\hbar = 1$ for convenience.

Now, we consider the dynamics of a electron spin precession in a reference frame following exactly the classical trajectory of the driven electron in a harmonic trap. To this end, we introduce a time-dependent displacement transformation [33]

$$D[f(t)] = e^{f(t)a^\dagger - \text{h.c.}} \equiv e^{-i[p_x x_c(t) + x p_c(t)]},$$ (2)

where $p_c(t) = m\dot{x}_c$ and

$$x_c(t) = -\sqrt{\frac{2}{m_e\omega}}\frac{\omega\xi}{\omega^2 - \nu^2}\cos\nu t,$$

corresponds to the classical trajectory of a driven harmonic oscillator (DHO) described by the classical Hamiltonian $\mathcal{H}_c$ (please refer to Eq. (A.8) in Appendix A for details). Here, $f(t) = -(\sqrt{m_e\omega/2}x_c + ip_c/\sqrt{2m_e\omega})$ represents a complex displacement in the phase space. As displayed in Appendix A, the above unitary transformation $D(t) = D[f(t)]$ is equivalent to the quantum linear coordinate transformation [34,35]

$$x' = x - x_c(t), \; t' = t, \; \nabla' = \nabla, \; \frac{\partial}{\partial t'} = \frac{\partial}{\partial t} + \dot{x}_c\nabla', \quad (3)$$

accompanied by a corresponding transformation of the wave function $\psi'(x',t') = \psi(x,t)\exp(-i\phi)$, with $\phi = [p_c x' + (1/m_e)\int_0^{t'} p_c^2(\tau)d\tau]$, as the requirement of covariance. The above transformation $D[f(t)]$ gives the equivalent Hamiltonian $H_D = DHD^\dagger - iD\left(\partial_t D^\dagger\right)$ in the reference frame moving along the classical path $x_c(t)$ as

$$H_D = \omega a^\dagger a - i\tilde{\alpha}(a^\dagger - a)\sigma_y - \eta\tilde{\alpha}\sigma_y\sin\nu t + \frac{1}{2}\omega_z\sigma_z. \quad (4)$$

Here, $\eta = 2\nu\xi/(\omega^2 - \nu^2)$ is a dimensionless parameter and we have neglected a time-dependent c-number $\mathcal{E}_c = -(\omega\xi^2\cos^2\nu t)/(\omega^2 - \nu^2)$, which corresponds to the classical energy of this DHO.

It is found that η is proportional to the driving strength ξ and will be greatly enhanced if the driving frequency ν is nearly resonant with the frequency of the trap ω. It follows Hamiltonian (4) that, in the new reference frame, the forced oscillation of the electron under the a.c. electric field induces a time-dependent spin flipping term with the same frequency as the electric field.

3 Effective spin precession

In experiment [21,22], the electron is tightly constrained in the trap with orbital transition energy $\sim$5–9 meV (corresponding oscillating frequency $\omega \sim 10^{12}$–10^{13} Hz), the SOC strength $\tilde{\alpha} \sim 10^9$ Hz, the Zeeman splitting ω_z is $\sim 10^{10}$ Hz with $B \sim 0.1$ T and $g \approx 9$, and the driving frequency ν is resonant with ω_z. Thus, we have the condition $\omega \gg \omega_z \approx \nu > \tilde{\alpha}$, and then we can adiabatically eliminate the degree of the freedom of the vibration part to obtain the effective spin Hamiltonian.

The formal solution of the Heisenberg equation of $a(t)$ reads

$$a(t) = a(0)e^{-i\omega t} - \tilde{\alpha}e^{-i\omega t} \int_0^t \sigma_y(\tau)e^{i\omega\tau}d\tau. \quad (5)$$

To estimate the value of the integral in equation (5), we first analyze the oscillatory behavior of $\sigma_y(t)$. In the case of $\omega \gg \omega_z \approx \nu > \tilde{\alpha}$, the SOC in equation (4) will contribute a fast oscillating term in the motion equation of the spin operators, and the strength of the resonant term $\eta\tilde{\alpha}$ is much smaller than the Zeeman splitting ω_z, i.e., $\eta\tilde{\alpha} \ll \omega_z$. Thus, the zeroth order of the spin operator $\sigma_y(t)$ is of $\sim \exp(\pm i\omega_z t)$, then the magnitude of the integral in equation (5) is approximated as $\tilde{\alpha}/(\omega \pm \omega_z) \ll 1$. As a result, the influence of the SOC on the dynamics of the vibration part can be neglected. Then we can take the semi-classical approximation by replacing a and $a^\dagger$ in Hamiltonian (4) with $\langle a(0)\rangle_D \exp(-i\omega t)$ and $\langle a^\dagger(0)\rangle_D \exp(i\omega t)$ ($\langle \cdots \rangle_D$ means averaging over the displaced initial state), respectively. For simplicity, we assume the system is in the state $|\psi(0)\rangle = |0\rangle \otimes |\uparrow\rangle$, and then the effective Hamiltonian for the spin part reads

$$H_s^{\text{eff}} = \frac{1}{2}\omega_z\sigma_z - \eta\tilde{\alpha}\sigma_y \sin\nu t + \frac{2\omega}{\nu}\eta\tilde{\alpha}\sigma_y \sin\omega t. \quad (6)$$

The free oscillation and the forced oscillation of the electron generate two effective a.c. magnetic fields $B_{\text{free}} = (2\omega/\nu)B_{\text{ind}}\sin\omega t$ and $B_{\text{E}} = -B_{\text{ind}}\sin\nu t$ for the spin, respectively, with $B_{\text{ind}} = \eta\tilde{\alpha}/(g\mu_B)$. The strengths of these two effective magnetic fields are both proportional to $\tilde{\alpha}\xi$. In a 1D case, the effective magnetic fields induced by Rashba SOC (both B_{free} and B_{E}) are perpendicular to the electric field, and the magnetic fields induced by the Dresselhaus SOC are parallel to the electric field.

We find that the effective magnetic field B_{E} generated by the forced oscillation of the electron under the electric field through SOC has the same frequency ν as the electric field. The effective field B_{free} generated by the free oscillation of the electron has the same frequency as the frequency of the harmonic trap ω. Although the strength of B_{free} is $2\omega/\nu$ times larger than B_{E}, it contributes little to the spin control because its frequency ω is largely detuning from ω_z. Therefore, in the case of $\omega \gg \omega_z \approx \nu > \tilde{\alpha}$, the dynamics of the spin can be described by the following Hamiltonian,

$$H_s^{\text{RWA}} = \frac{1}{2}\omega_z\sigma_z - \frac{\eta\tilde{\alpha}}{2}\left(\sigma_+e^{-i\nu t} + \sigma_-e^{i\nu t}\right). \quad (7)$$
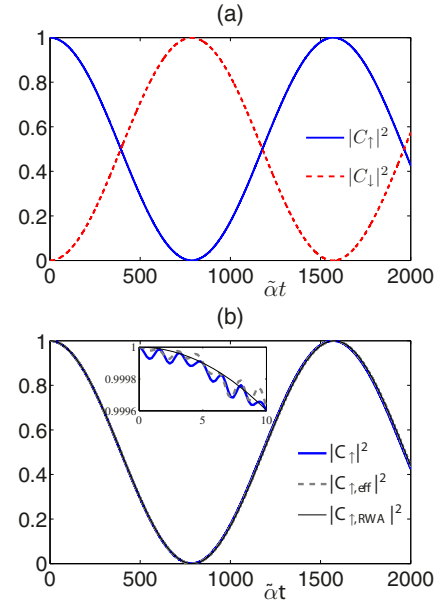
Fig. 2. We take the SOC constant as the unit $\tilde{\alpha} = 1$. $\omega = 250$, $\omega_z = 2.5$, $\nu = 2.5$, and $\xi = 50$. (a) The solid blue (dashed red) line is the probability of the $|\uparrow\rangle$ ($|\downarrow\rangle$) state of the spin, which is directly calculated via H_D. (b) Probabilities of the spin state $|\uparrow\rangle$ obtained by different methods are presented. The solid blue line is obtained from the numerical calculation via H_D. The dashed gray line is obtained from H_s^{eff}. And the thin black line is obtained from H_s^{RWA} with rotating wave approximation.

Here, we have neglected the influence of the fast oscillating term B_{free} and taken the rotating approximation (RWA) of the resonant term associated with B_{E}.

To demonstrate the coherent control of the electron spin, we turn to numerical calculations. The spin is initially polarized in the state $|\uparrow\rangle$ and its wave function at time t can be expanded as $|\chi(t)\rangle = C_\uparrow(t)|\uparrow\rangle + C_\downarrow(t)|\downarrow\rangle$. Here, $|C_\uparrow(t)|^2$ ($|C_\downarrow(t)|^2$) denotes the occupation probability of the state $|\uparrow\rangle$ ($|\downarrow\rangle$). In the case of $\omega \gg \omega_z = \nu > \tilde{\alpha}$, the perfect Rabi oscillation of the spin with frequency $\eta\tilde{\alpha} \sim (10^{-4}$–$10^{-3})\tilde{\alpha}$ is observed when the driving frequency ν is resonant with ω_z as shown in Figure 2a. In Figure 2b, the solid blue line is obtained directly from the Hamiltonian H_D by tracing off the degree of freedom of the vibration, the dashed gray line is obtained from H_s^{eff}, and thin black line is obtained from H_s^{RWA}. These three lines coincide with each other very well, except for some high-frequency fluctuation around the thin black line (obtained from H_s^{RWA}) as shown in the subgraph of Figure 2b. Thus, the dynamics of the spin is well described by H_s^{RWA} in the regime $\omega \gg \omega_z = \nu > \tilde{\alpha}$. Similar to ESR, the electron spin could be well controlled with electric field via EDSR.

4 Coherent-spin-control speed enhancement

In the preceding sections, we found that one can coherently control the electric spin with electric field through EDSR just like with magnetic field. Next, we will explore
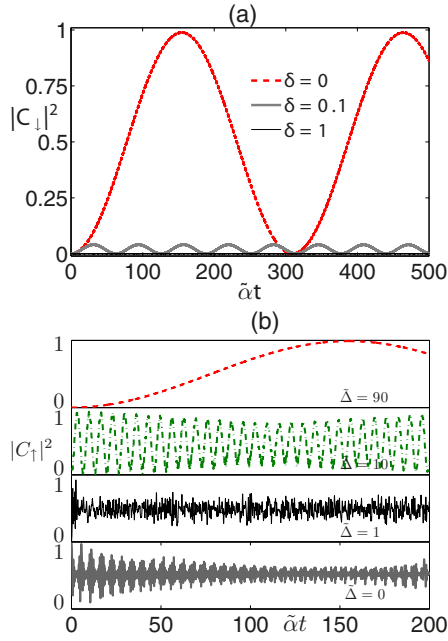
Fig. 3. Here, we take the SOC strength as the unit $\alpha = 1$. (a) The flipping probabilities for different detunings δ between the driving electric field and the Zeeman splitting of the electron spin are presented. The parameters are taken as $\omega = 100$, $\omega_z = 10$, $\xi = 10$. The dotted red line described the resonant case with $\nu = \omega_z$, $\delta = 0$ and $\eta = 0.0202$. The solid gray line described the case with $\nu = 9.9$, $\delta = 0.1$ and $\eta = 0.02$. The thin black line described the large detuning case with $\nu = 9$, $\delta = 1$ and $\eta = 0.0181$. (b) The flipping probabilities for different detunings $\tilde{\Delta}$ between frequency of the harmonic well and the Zeeman splitting of the electron spin are presented. Here, $\omega = 100$, $\xi = 10$, and the resonance condition $\delta = 0$ is always guaranteed. And the other parameters are: $\nu = \omega_z = 10$ with $\tilde{\Delta} = 90$ for the dotted red line, $\nu = \omega_z = 90$ with $\tilde{\Delta} = 10$ for the dash-dotted green line, $\nu = \omega_z = 99$ with $\tilde{\Delta} = 1$ for the thin black line, $\nu = \omega_z = 100$ with $\tilde{\Delta} = 0$ for the solid gray line.

how to speed up coherent spin control with EDSR. First, we give the conditions to realize coherent control of electron spin with EDSR. For a spin-1/2 system described by Hamiltonian (7), the flipping probability $|C_\downarrow(t)|^2$ for the Rabi oscillation reads

$$|C_\downarrow(t)|^2 = \frac{(\eta\tilde{\alpha})^2}{\delta^2 + (\eta\tilde{\alpha})^2} \sin^2\left(\sqrt{\delta^2 + (\eta\tilde{\alpha})^2}\, t/2\right), \qquad (8)$$

where $\delta = \omega_z - \nu$ is the detuning between the driven frequency and the Zeeman splitting of the electron spin. As shown in Figure 3a, the amplitude of the Rabi oscillation tends to 1 when $\delta \ll \eta\tilde{\alpha}$, while the amplitude tends to 0 when $\delta \gg \eta\tilde{\alpha}$. As a result, the flipping probability is deeply suppressed by the detuning δ.

Similarly, when the detuning between the frequencies of harmonic trap and the Zeeman splitting $\tilde{\Delta} = \omega - \omega_z \gg \omega\eta\tilde{\alpha}/\nu$ is large, the effective magnetic field B_{free} hardly affects the spin-flipping process. As a result, the influence of the free oscillation of the electron on the dynamics of the spin can be neglected in the former section.

In addition, the "fractional-frequency EDSR" effect has recently been discovered [36–39], in which the frequency of the a.c. electric field ν is a fraction of the Zeeman splitting of the spin $g\mu_B B$ (i.e., $\nu = g\mu_B B/n$, n is a positive integer) instead of being resonant with it. Actually, the "fractional-frequency EDSR" is another different resonance mechanism. The core of this effect lies in that the induced a.c. magnetic field has one component parallel to the static magnetic field. This component does not flip the spin but changes its energy splitting frequently. When the frequency of the a.c. magnetic field satisfies $\nu = g\mu_B B/n$, a resonance occurs [40]. A similar method was used to control the coupling and its surroundings [41].

Starting from the original Hamiltonian (1), we numerically study the influence of the detuning $\tilde{\Delta}$ to the coherent controlling of the spin. It is discovered that when $\tilde{\Delta} \gg \tilde{\alpha}$ and $\delta \ll \eta\tilde{\alpha}$, the coherent controlling of electron spin is realized, as shown by the dotted red line ($\tilde{\Delta} = 90\tilde{\alpha}$) in Figure 3b. When $\tilde{\Delta} \lesssim \tilde{\alpha}$, the SOC will destroy the coherence of the spin, and then collapse and revival phenomenon appear. As shown by the thin black line ($\tilde{\Delta} = 1\tilde{\alpha}$) and the solid gray line $\tilde{\Delta} = 0$ in Figure 3b, the coherent controlling of the electron spin is destroyed by SOC. As a result, to realize perfect spin control through EDSR, two necessary conditions must be guaranteed: (1) the frequency of the a.c. electric field must be resonant with the Zeeman splitting of the spin in the external magnetic field, i.e., $\delta \ll \eta\tilde{\alpha}$; (2) the frequency of the harmonic trap must be largely detuned from the Zeeman splitting of the spin, i.e., $|\tilde{\alpha}/\tilde{\Delta}| \ll 1$.

According to equation (8), spin-flip speed is characterized by the Rabi frequency:

$$\Omega_R = \frac{1}{2}\eta\tilde{\alpha} = \frac{\omega_z\xi\tilde{\alpha}}{\omega^2 - \omega_z^2}, \qquad (9)$$

where we have used the resonance condition $\delta = \omega_z - \nu = 0$. It is found that this Rabi frequency Ω_R is proportional to the strengths of the SOC $\tilde{\alpha}$ and electric driving ξ. Hence, we should increase $\tilde{\alpha}$ and ξ to enlarge Ω_R. But if the driving strength $\xi \gg \omega$, the electron will flee from the harmonic trap. When $\tilde{\alpha}$ is large enough to break the large detuning condition $|\tilde{\alpha}/\tilde{\Delta}| \ll 1$, the free oscillation of the electron and the spin precession will be highly correlated, thus the SOC will destroy the coherent control according to Hamiltonian (4). For safety, we require $\xi \leqslant \omega$ and $0 < |\tilde{\alpha}/\tilde{\Delta}| \leqslant 0.01$ to guarantee the perfect Rabi oscillation of the electron spin in the trap. From equation (9), Ω_R monotonically increases with ω_z with an upper limit of $10^{-2}\omega_z$ for this case (see Fig. 4). Thus, for a very large ω, one can increase ω_z, besides the driving strength ξ and SOC strength $\tilde{\alpha}$, to speed up the spin flipping.

5 Two-dimensional quantum dot system

For the two-dimensional (2D) QD system, the magnetic field induced by the a.c. electric field via SOC becomes azimuth-dependent and much more complicated. We can utilize this azimuth dependence to measure the Rashba
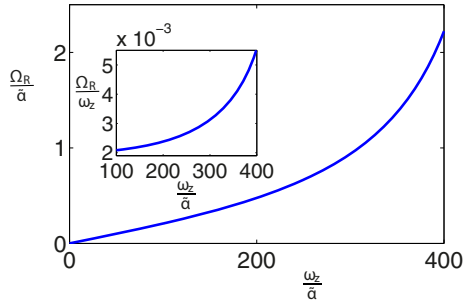
Fig. 4. Here, we take the SOC strength as the unit $\alpha = 1$. The Rabi frequency of the coherence spin flip increases with ω_z. The parameters are taken as $\xi = \omega = 500$.

and Dresselhaus SOC strength ratio and realize a perfect single electron spin qubit operation through EDSR.

The Hamiltonian of the electron confined in a 2D harmonic trap $H = H_v + H_s + H_{so} + V(t)$ is composed of four parts: the vibration part of the electron is described with

$$H_v = \frac{1}{2m_e}\left[\boldsymbol{p} + \frac{e}{c}\boldsymbol{A}(\boldsymbol{r})\right]^2 + \frac{1}{2}m_e\tilde{\omega}_x^2 x^2 + \frac{1}{2}m_e\tilde{\omega}_y^2 y^2, \quad (10)$$

where $\boldsymbol{p} = p_x\boldsymbol{e}_x + p_y\boldsymbol{e}_y$ is the in-plane momentum, $\tilde{\omega}_{x(y)}$ the frequency of the harmonic trap of $x(y)$-direction, and $\boldsymbol{A}(\boldsymbol{r}) = B(0, 0, y\cos\varphi_B - x\sin\varphi_B)$ the vector potential for the in-plane static magnetic field $\boldsymbol{B} = B(\cos\varphi_B, \sin\varphi_B, 0)$. The second part $H_s = \hbar g\mu_B \boldsymbol{B} \cdot \boldsymbol{\sigma}/2$ describes the Zeeman splitting of the electron spin in $\boldsymbol{B} = B(\cos\varphi_B, \sin\varphi_B, 0)$. For the third part, both the Rashba and Dresselhaus SOC with strength α_R and α_D, respectively, are taken into account

$$H_{so} = \alpha_R(\sigma_x p_y - \sigma_y p_x) + \alpha_D(\sigma_y p_y - \sigma_x p_x). \quad (11)$$

The last part $V(t) = -e\boldsymbol{r} \cdot \boldsymbol{E}(t)$ describes the in-plane electric drive with $\boldsymbol{E}(t) = -(E\boldsymbol{e}_x\cos\varphi_E + E\boldsymbol{e}_y\sin\varphi_E)\cos\nu t$.

After a unitary transformation similar to the 1D case, the a.c. electric field will be converted to an a.c. magnetic field with the same frequency (please refer to Appendix B for details). In the experiment [18], the external static magnetic field is weak, i.e., the frequency modification induced by the vector potential can be neglected $\omega_c = eB/(m_e c) \ll \tilde{\omega}_{x(y)}$ [42]. In this case, the effective spin Hamiltonian for the isotropic 2D harmonic well $\tilde{\omega}_x = \tilde{\omega}_y = \omega$ could be simplified to

$$H_s^{\text{eff}} = \frac{1}{2}g\mu_B\left[\boldsymbol{B} + \boldsymbol{B}_R(t) + \boldsymbol{B}_D(t)\right] \cdot \boldsymbol{\sigma}, \quad (12)$$

where

$$\boldsymbol{B}_R(t) = B_R\sin\nu t(\sin\varphi_E, -\cos\varphi_E, 0)$$

and $\boldsymbol{B}_D(t) = B_D\sin\nu t(-\cos\varphi_E, \sin\varphi_E, 0)$ are the magnetic fields induced by Rashba and Dresselhaus SOC respectively, with strength

$$B_{R(D)}(t) = \frac{2\hbar\nu e E\alpha_{R(D)}}{g\mu_B(\omega^2 - \nu^2)}. \quad (13)$$
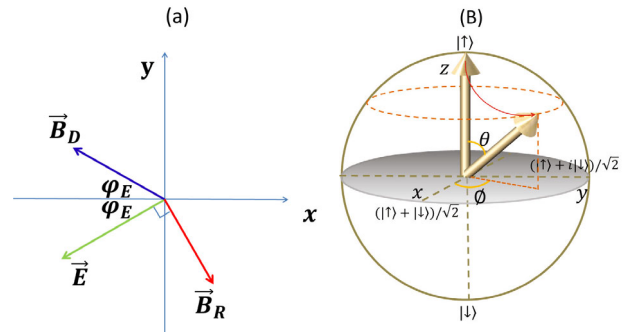
Fig. 5. The 2D electric field caused spin precession on the Bloch sphere. (a) Schematic of the directions of the induced magnetic fields. (b) The trajectory of the spin from the initial point $\rho(0) = |\uparrow\rangle\langle\uparrow|$ to the final state $\rho(\theta, \phi)$ with $\theta = g\mu_B B_R t/2$ and $\phi = \nu t + \varphi_E$ on the Bloch sphere surface.

It is observable that $\boldsymbol{B}_R$ is always vertical to the electric field $\boldsymbol{E}$, but that $\boldsymbol{B}_D$ is vertical to $\boldsymbol{E}$ only when the polarization angle of the electric field is $\varphi_E = n\pi/2 + \pi/4$ ($n = 0, 1, 2, 3$) (see Fig. 5a). When $\varphi_E = 3\pi/4$ or $7\pi/4$, $\boldsymbol{B}_R$ and $\boldsymbol{B}_D$ are parallel, $\boldsymbol{B}_R$ and $\boldsymbol{B}_D$ are anti-parallel when $\varphi_E = \pi/4$ or $5\pi/4$. Therefore, one can measure the ratio of the SOC strength α_R/α_D by measuring the different Rabi frequencies for $\varphi_E = \pi/4$ and $\varphi_E = 3\pi/4$ [15].

In addition, the direction of the effective magnetic field can be controlled by tuning the direction of the a.c. electronic field. For the case where the static magnetic field along z-direction $\boldsymbol{B} = B(0, 0, 1)$ instead of the in-plane one is applied, the induced magnetic fields are nearly the same. If there is only one type of SOC (e.g., Rashba one), we can use the electric field to induce an effective magnetic field in any needed direction, which controls the evolution of the spin state from a starting point to anywhere we wanted on the Bloch sphere. If the electric field is resonant with the Zeeman splitting of the spin (i.e., $\nu = g\mu_B B$, the dynamics of the spin can be described by the Hamiltonian

$$H_s^{RWA} = \frac{g\mu_B}{2}B\sigma_z - \frac{B_R}{2}\left[e^{-i(\varphi_E + \nu t)}\sigma_+ + e^{i(\varphi_E + \nu t)}\sigma_-\right]. \quad (14)$$

An arbitrary target state $\rho(\theta, \phi) = (1 + \boldsymbol{n} \cdot \boldsymbol{\sigma})/2$ with $\boldsymbol{n} = (\sin\theta\cos\phi, \sin\theta\sin\phi, \cos\theta)$ on the Bloch sphere can be realized through EDSR by choosing proper time $g\mu_B B_R t/2 = \theta$ and proper angle $\varphi_E = \phi - \nu t$ from the starting point $\rho_0 = |\uparrow\rangle\langle\uparrow|$ (see Fig. 5b). Namely, the electric field can perform a perfect single-qubit operation in the spin system through EDSR.

6 Summary

For the physical mechanism of EDSR in 1D nanowire QD or for a 2D case, we provide an intuitive explanation with an exact picture in physics based on the reference frame transformation: the electric field can behave as a magnetic field in the reference frame following exactly the classical trajectory of a DHO. This electric-magnetic duality can

generally be found in the relativistic transformation of Maxwell equations. We also notice that SOC is in essence the consequence of relativistic quantum theory in the low-velocity limit. Thus our approach presented in this paper is, in principle, consistent with the point of view of special relativity.

For the EDSR technology itself, our study shows that two necessary conditions must be guaranteed to realize perfect spin control through EDSR: (1) the frequency of the a.c. electric field must be resonant with the Zeeman splitting of the spin; (2) the detuning beween the frequency of the harmonic trap and the Zeeman splitting of the spin must be much larger than SOC coupling strength. Based on these conditions, there are three ways to increase the speed of coherent spin control: (1) increasing the electric driving strength; (2) increasing the strength of SOC $\tilde{\alpha}$; (3) increasing the external state magnetic field to increase the Zeeman splitting of the electron spin.

The azimuthal dependence of the induced magnetic field can be used to measure the ratio of the strengths of the Rashba and Dresselhaus SOC. We also show that the precise control of spin in the whole Bloch sphere can be realized in 2D QD systems through EDSR technology.

Appendix A: The quantum driven harmonic oscillator

A.1 Time-dependent displacement transformation

The exact solution of the Schrödinger equation of a quantum driven harmonic oscillator (DHO) described by Hamiltonian

$$H = \omega a^\dagger a + [F(t)a + \text{h.c.}], \tag{A.1}$$

has been given by Husimi [43] in 1953 (and independently by Kerner [44] in 1958). Here, we give another method to deal this problem by taking a time-dependent displacement transformation

$$D[f(t)] = \exp\left[f(t)a^\dagger - f^*(t)a\right], \tag{A.2}$$

where function $f(t)$ is to be determined. It is ready to find the relations

$$DaD^\dagger = a - f(t), \text{ and } Da^\dagger D^\dagger = a^\dagger - f^*(t). \tag{A.3}$$

After the transformation, the effective Hamiltonian reads

$$\tilde{H} = DHD^\dagger - iD\left(\frac{\partial}{\partial t}D^\dagger\right). \tag{A.4}$$

One finds that the Hamiltonian will be diagonalized if we choose suitable function $f(t)$ satisfying

$$\omega f - F^* - i\dot{f} = 0, \tag{A.5a}$$

$$\omega f^* - F + i\dot{f}^* = 0. \tag{A.5b}$$

Now we split $f(t)$ into real and imaginary parts

$$f(t) = -\left(\sqrt{\frac{m_e\omega}{2}}x_c + i\sqrt{\frac{1}{2m_e\omega}}p_c\right). \tag{A.6}$$

Then equations (A.5a) and (A.5b) change into

$$\dot{p}_c = -\left[m\omega^2 x_c + \sqrt{\frac{m_e\omega}{2}}(F + F^*)\right], \tag{A.7a}$$

$$\dot{x}_c = \frac{p_c}{m} + i\sqrt{\frac{1}{2m_e\omega}}(F - F^*). \tag{A.7b}$$

If F is real, it is observable that x_c and p_c satisfy the classical Hamilton equation generated by the classical Hamiltonian of a forced classical harmonic oscillator

$$\mathcal{H}_c = \frac{p_c^2}{2m_e} + \frac{1}{2}m_e\omega^2 x_c^2 + \tilde{F}(t)x_c, \tag{A.8}$$

with $\tilde{F}(t) = \sqrt{2m_e\omega}F(t)$.

In our case $F = F^* = \xi\cos\nu t$, then we obtain the solution

$$x_c(t) = -\sqrt{\frac{2}{m_e\omega}}\frac{\omega\xi}{\omega^2 - \nu^2}\cos\nu t + A\sin\omega t + B\cos\omega t, \tag{A.9}$$

$$p_c(t) = \sqrt{2m_e\omega}\frac{\nu\xi}{\omega^2 - \nu^2}\sin\nu t + A\omega\cos\omega t - B\omega\sin\omega t, \tag{A.10}$$

where A and B are time-independent constants. For simplicity, we take $A = B = 0$ (corresponding to the special initial conditions $x_c(0) = -\sqrt{2\omega/m_e}\xi/(\omega^2 - \nu^2)$ and $\dot{x}_c(0) = 0$), then the displacement operator reads

$$D = e^{-i[px_c(t) + xp_c(t)]}, \tag{A.11}$$

and the Hamiltonian changes into

$$H_D = \omega a^\dagger a + \mathcal{E}_c, \tag{A.12}$$

where

$$\mathcal{E}_c = -\frac{\omega\xi^2}{\omega^2 - \nu^2}\cos^2\nu t. \tag{A.13}$$

As shown in the following subsection, $\mathcal{E}_c$ corresponds to the classical energy for the DHO.

A.2 Equivalent quantum coordinate transformation

In this subsection, it will be shown that the time-dependent unitary transformation in the former subsection corresponds to a quantum linear coordinate transformation [43,45].

Now, we rewrite the Hamiltonian of the DHO as:

$$H = -\frac{\hbar^2}{2m_e}\nabla^2 + \frac{1}{2}m_e\omega^2 x^2 + \tilde{F}(t)x. \tag{A.14}$$

Then we take a linear coordinate-translation transformation

$$x' = x - x_c(t),\qquad (A.15)$$

where the time-dependent c-number $x_c(t)$ satisfies the classical Hamilton equation

$$\dot{x}_c = \frac{p_c}{m_e},\qquad (A.16a)$$

$$\dot{p}_c = -m_e\omega^2 x_c - \tilde{F}(t),\qquad (A.16b)$$

i.e.,

$$m_e\ddot{x}_c + m_e\omega^2 x_c + \tilde{F}(t) = 0.\qquad (A.17)$$

Obviously, $x_c(t)$ describes the classical path of the DHO. It is ready to obtain the following relations

$$x' = x - x_c(t),\ t' = t,\ \nabla' = \nabla,\ \frac{\partial}{\partial t'} = \frac{\partial}{\partial t} + \dot{x}_c\nabla'.\ (A.18)$$

As the consequence of the required covariance,

$$i\hbar\frac{\partial}{\partial t'}\psi'(x',t') = H'\psi'(x',t'),\qquad (A.19)$$

a transformation of the wave function is needed

$$\psi'(x',t') = \psi(x,t)e^{-i\phi},\qquad (A.20)$$

with

$$\phi = \frac{1}{\hbar}\left[p_c x' + \frac{1}{m_e}\int_0^{t'} p_c^2(\tau)d\tau\right].\qquad (A.21)$$

Here, the Hamiltonian in the new reference frame reads

$$H' = -\frac{\hbar^2}{2m}\nabla'^2 + \frac{1}{2}m\omega^2 x'^2 + \mathcal{H}_c(t),\qquad (A.22)$$

where $\mathcal{H}_c(t) = (p_c^2/m_e + m_e\omega^2 x_c^2)/2 + \tilde{F}(t')x_c$ is the classical Hamiltonian of the DHO. It is found that the DHO moves as a free harmonic oscillator in this new reference frame.

For our case $F = \hbar\xi\cos\nu t$, we also take the solution of the Hamilton equation (A.17) as

$$x_c(t) = -\sqrt{\frac{2\omega}{\hbar m_e}}\frac{\xi\cos\nu t'}{\omega^2 - \nu^2}.\qquad (A.23)$$

Following the classical Hamiltonian $\mathcal{H}_c(t)$, we obtain the classical energy of the DHO

$$\mathcal{E}_c(t') = -\frac{\omega\xi^2}{\omega^2 - \nu^2}\cos^2\nu t',\qquad (A.24)$$

which is the exact time-dependent function defined in equation (A.13). It should be pointed that we have neglected a time-independent constant $\omega\xi^2\nu^2/(\omega^2 - \nu^2)^2$ and taken $\hbar = 1$ in equation (A.22). Consequently, this quantum linear coordinate transformation is equivalent with the time-dependent displacement $D(t)$ defined in equation (A.2).

Appendix B: Two-dimensional quantum dot system

B.1 Diagonalization of the vibration potential

By defining creation and annihilation operators

$$x = \frac{1}{\sqrt{2m_e\omega_x}}\left(a^\dagger + a\right),\ y = \frac{1}{\sqrt{2m_e\omega_y}}\left(b^\dagger + b\right),\quad (B.1)$$

we rewrite the vibration Hamiltonian (10) of the electron in 2D QD system as

$$H_v = \omega_x a^\dagger a + \omega_y b^\dagger b - \chi\left(a^\dagger b + ab^\dagger\right)$$

where

$$\omega_x^2 = \tilde{\omega}_x^2 + \omega_c^2\sin^2\varphi_B,\qquad (B.2)$$

$$\omega_y^2 = \tilde{\omega}_y^2 + \omega_c^2\cos^2\varphi_B,\qquad (B.3)$$

$$\omega_c = \frac{eB}{m_e c},\qquad (B.4)$$

and we have taken the rotating wave approximation since

$$\chi = \omega_c\sin 2\varphi_B\sqrt{\frac{\omega_c^2}{\omega_x\omega_y}} \ll \omega_{x(y)}.\qquad (B.5)$$

Hereafter, we let $\hbar = 1$ for simplicity.

It is convenient to diagonalize H_v by defining two new modes,

$$\begin{pmatrix} A \\ B \end{pmatrix} = \begin{pmatrix} \cos\frac{\vartheta}{2} & -\sin\frac{\vartheta}{2} \\ \sin\frac{\vartheta}{2} & \cos\frac{\vartheta}{2} \end{pmatrix}\begin{pmatrix} a \\ b \end{pmatrix},\qquad (B.6)$$

where

$$\cos\vartheta = \frac{\Delta/2}{\sqrt{\Delta^2/4 + \chi^2}},\ \sin\vartheta = \frac{\chi}{\sqrt{\Delta^2/4 + \chi^2}},\quad (B.7)$$

and $\Delta = \omega_x - \omega_y$. Then the H_v changes into

$$H_v = \omega_A A^\dagger A + \omega_B B^\dagger B,\qquad (B.8)$$

with the frequencies,

$$\omega_{A(B)} = \frac{\omega_x + \omega_y}{2} \pm \sqrt{\frac{\Delta^2}{4} + \chi^2}.\qquad (B.9)$$

The effective driving for the the new two modes reads

$$V(t) = \xi_A\left(A^\dagger + A\right)\cos\nu t + \xi_B\left(B^\dagger + B\right)\cos\nu t,\quad (B.10)$$

with corresponding driving strength,

$$\xi_A = \frac{eE}{\sqrt{2m_e}}\left[\frac{1}{\sqrt{\omega_x}}\cos\frac{\vartheta}{2}\cos\varphi_E - \frac{1}{\sqrt{\omega_y}}\sin\frac{\vartheta}{2}\sin\varphi_E\right],$$
$$(B.11)$$

$$\xi_B = \frac{eE}{\sqrt{2m_e}}\left[\frac{1}{\sqrt{\omega_x}}\sin\frac{\vartheta}{2}\cos\varphi_E + \frac{1}{\sqrt{\omega_y}}\cos\frac{\vartheta}{2}\sin\varphi_E\right].$$
$$(B.12)$$

B.2 Effective spin-controlling Hamiltonian

Just like the one-dimensional case, we take a similar unitary transformation

$$D[t] = \exp\left[f_A(t)A^\dagger + f_B(t)B^\dagger\right] - \text{h.c.}, \qquad (B.13)$$

where

$$f_A = \frac{\xi_A}{\omega_A^2 - \nu^2}(\omega\cos\nu t - i\nu\sin\nu t), \qquad (B.14)$$

$$f_B = \frac{\xi_B}{\omega_B^2 - \nu^2}(\omega\cos\nu t - i\nu\sin\nu t). \qquad (B.15)$$

Then the Hamiltonian changes into $H = H_v + H_s + H_{so} + H_{flip}$, where

$$H_{flip} = [G_1(\alpha_R\sigma_x + \alpha_D\sigma_y) - G_2(\alpha_R\sigma_y + \alpha_D\sigma_x)]\sin\nu t, \qquad (B.16)$$

with

$$G_1 = \frac{1}{2}\eta_B\left(\sqrt{\frac{\omega_y}{\omega_x}}\sin\frac{\vartheta}{2}\cos\frac{\vartheta}{2}\cos\varphi_E + \cos^2\frac{\vartheta}{2}\sin\varphi_E\right) - \frac{1}{2}\eta_A\left(\sqrt{\frac{\omega_y}{\omega_x}}\sin\frac{\vartheta}{2}\cos\frac{\vartheta}{2}\cos\varphi_E - \sin^2\frac{\vartheta}{2}\sin\varphi_E\right), \qquad (B.17)$$

$$G_2 = \frac{1}{2}\eta_B\left(\sqrt{\frac{\omega_x}{\omega_y}}\sin\frac{\vartheta}{2}\cos\frac{\vartheta}{2}\sin\varphi_E + \sin^2\frac{\vartheta}{2}\cos\varphi_E\right) - \frac{1}{2}\eta_A\left(\sqrt{\frac{\omega_x}{\omega_y}}\sin\frac{\vartheta}{2}\cos\frac{\vartheta}{2}\sin\varphi_E - \cos^2\frac{\vartheta}{2}\cos\varphi_E\right). \qquad (B.18)$$

Here, the additional spin-flipping term H_{flip} is generated by the electric field mediated by SOC and

$$\eta_{A(B)} = \frac{2\nu eE}{\omega_{A(B)}^2 - \nu^2}. \qquad (B.19)$$

For most cases, the azimuthal dependence of H_{flip} about φ_E is complicate. In experiment, the external static magnetic field is weak $\chi \ll \omega$, and so the influence of the vector potential $\boldsymbol{A}(\boldsymbol{r})$ can be neglected, i.e., $\vartheta \to 0$ and $\omega_{A(B)} \approx \tilde{\omega}_{x(y)}$. If the 2D harmonic well is isotropic $\tilde{\omega}_x = \tilde{\omega}_y = \omega$, one will get the effective spin Hamiltonian (12).

References

1. R. Hanson, L.P. Kouwenhoven, J.R. Petta, S. Tarucha, L.M.K. Vandersypen, Rev. Mod. Phys. **79**, 1217 (2007)
2. R. Hanson et al., Phys. Rev. Lett. **94**, 196802 (2005)
3. W. van Berveren, New J. Phys. **7**, 182 (2005)
4. J. Berezovsky, M.H. Mikkelsen, N.G. Stoltz, L.A. Coldren, D.D. Awschalom, Science **320**, 349 (2008)
5. S. Nadj-Perge et al., Phys. Rev. B **81**, 201305 (2010)
6. S. Hermelin et al., Nature **477**, 435 (2011)
7. R.P.G. McNeil et al., Nature **477**, 439 (2011)
8. M. Kataoka et al., Phys. Rev. Lett. **106**, 126801 (2011)
9. S.A. Wolf et al., Science **294**, 1488 (2001)
10. D. Awschalom, D. Loss, N. Samarth, *Semiconductor Spintronics and Quantum Computation* (Springer-Verlag, Berlin, 2002)
11. C.P. Poole, *Electron Spin Resonance*, 2nd edn. (Wiley, New York, 1983)
12. F.H.L. Koppens et al., Nature **442**, 766 (2006)
13. D. Press et al., Nature **456**, 218 (2008)
14. E.I. Rashba, Al.L. Efros, Phys. Rev. Lett. **91**, 126405 (2003)
15. E.I. Rashba, Al.L. Efros, Appl. Phys. Lett. **83**, 5295 (2003)
16. G. Dresselhaus, Phys. Rev. **100**, 580 (1955)
17. Y.A. Bychkov, E.I. Rashba, J. Phys. C **17**, 6039 (1984)
18. K.C. Nowack et al., Science **318**, 1430 (2007)
19. E.A. Laird et al., Phys. Rev. Lett. **99**, 246601 (2007)
20. M. Pioro-Ladrière et al., Nat. Phys. **4**, 776 (2008)
21. S. Nadj-Perge et al., Nature **468**, 1084 (2010)
22. S. Nadj-Perge et al., Phys. Rev. Lett. **108**, 166801 (2012)
23. M. Shafiei, K.C. Nowack, C. Reichl, W. Wegscheider, L.M.K. Vandersypen, Phys. Rev. Lett. **110**, 107601 (2013)
24. E.I. Rashba, V.I. Sheka, in *Landau Level Spectroscopy* (North-Holland, Amsterdam, 1991), p. 131
25. V.N. Golovach, M. Borhani, D. Loss, Phys. Rev. B **74**, 165319 (2006)
26. E.I. Rashba, Phys. Rev. B **78**, 195302 (2008)
27. S. Bednarek, J. Pawlowski, A. Skubis, Appl. Phys. Lett. **100**, 203103 (2012)
28. R. Li, J.Q. You, C.P. Sun, F. Nori, Phys. Rev. Lett. **111**, 086805 (2013)
29. Y.N. Fang, Y. Turek, J.Q. You, C.P. Sun, Eur. Phys. J. B **87**, 140 (2014)
30. D.V. Khomitsky, L.V. Gulyaev, E.Y. Sherman, Phys. Rev. B **85**, 125312 (2012)
31. Y.V. Pershin, J.A. Nesteroff, V. Privman, Phys. Rev. B **69**, 121306 (2004)
32. C. Flindt, A.S. Sørensen, K. Flensberg, Phys. Rev. Lett. **97**, 240501 (2006)
33. T. Čadež, J.H. Jefferson, A. Ramšak, New J. Phys. **15**, 013029 (2013)
34. J.-M. Levy-Leblond, Commun. Math. Phys. **6**, 286 (1967)
35. G. Rosen, Am. J. Phys. **40**, 683 (1972)
36. E.A. Laird et al., Semicond. Sci. Technol. **24**, 064004 (2009)
37. S. Nadj-Perge et al., Phys. Rev. Lett. **108**, 166801 (2012)
38. M.P. Nowack, B. Szafran, F.M. Peeters, Phys. Rev. B **86**, 125428 (2012)
39. J. Stehlik et al., Phys. Rev. Lett. **112**, 227601 (2014)
40. E.I. Rashba, Phys. Rev. B **84**, 241305 (2011)
41. L. Zhou, S. Yang, Y.-X. Liu, C.P. Sun, F. Nori, Phys. Rev. A **80**, 062109 (2009)
42. N. Zhao, L. Zhong, J.-L. Zhu, C.P. Sun, Phys. Rev. B **74**, 075307 (2006)
43. K. Husimi, Prog. Theor. Phys. **4**, 381 (1953)
44. E.H. Kerner, Can. J. Phys. **36**, 371 (1958)
45. G. Rosen, Am. J. Phys. **40**, 683 (1972)